Arthropod Structure & Development 73 (2023) 101251

Contents lists available at ScienceDirect

Arthropod Structure & Development

journal homepage: www.elsevier.com/locate/asd

Investigation of the ultrastructures and retinal arrangements of larval stomatopod eyes

Marisa S. McDonald [a, 1, *], Kathryn D. Feller [b], Megan L. Porter [a]

[a] School of Life Sciences, 2538 McCarthy Mall, Edmondson Hall 216, University of Hawai'i at Mānoa, Honolulu, HI, 96822, USA
[b] Biology Department, Integrated Science and Engineering Complex 319, Union College, Schenectady, NY, 12308, USA

ARTICLE INFO

Article history:
Received 27 October 2022
Received in revised form
21 February 2023
Accepted 22 February 2023
Available online xxx

Handling Editor: Dr G. Scholtz

Keywords:
Transmission electron microscopy
Rhabdom
Stomatopod
Larvae
Ultraviolet

ABSTRACT

Though the transparent apposition eyes of larval stomatopod crustaceans lack most of the unique retinal specializations known from their adult counterparts, increasing evidence suggests that these tiny pelagic organisms possess their own version of retinal complexity. In this paper, we examined the structural organization of larval eyes in six species of stomatopod crustaceans across three stomatopod superfamilies using transmission electron microscopy. The primary focus was to examine retinular cell arrangement of the larval eyes and characterize the presence of an eighth retinular cell (R8), which is typically responsible for UV vision in crustaceans. For all species investigated, we identified R8 photoreceptor cells positioned distal to the main rhabdom of R1-7 cells. This is the first evidence that R8 photoreceptor cells exist in larval stomatopod retinas, and among the first identified in any larval crustacean. Considering recent studies that identified UV sensitivity in larval stomatopods, we propose that this sensitivity is driven by this putative R8 photoreceptor cell. Additionally, we identified a potentially unique crystalline cone structure in each of the species examined, the function of which is still not understood.

1. Introduction

Stomatopod crustaceans are well known for their unique and specialized visual systems, which are sensitive to an unparalleled range of wavelengths (including ultraviolet, UV) and e-vector orientations of polarized light (both linear and circular). A large portion of this visual complexity is driven by unique optical structures and photoreceptor arrangements in the adult eye (Marshall et al., 1991a, 1991b; Schiff et al., 2007; Bok et al., 2015, 2018, Thoen et al., 2017). Considering only specializations for UV vision, adult stomatopods possess one of the most complex and elaborate sets of sensitivities known for wavelengths shorter than 400 nm (Marshall and Oberwinkler, 1999; Cronin et al., 2014; Bok et al., 2015, 2018; Porter et al., 2020). Adult stomatopod UV sensitivity arises from the R8 cell type, a specialized retinular cell positioned in the distal part of the light-sensitive rhabdom. The majority of a typical crustacean rhabdom is formed by the microvilli projected from seven retinular cells (R1-7). In crustaceans, adult R1-7 cells provide sensitivity to blue or green wavelengths of light (~450 nm–550 nm wavelengths; Fig. 1A) (Marshall et al., 2015), although this range is expanded in mantis shrimp (~400–700 nm) (Thoen et al., 2014, 2017; Porter et al., 2020). Among most crustacean species, including stomatopods, the microvilli projected from the distally positioned R8 cell provides a separate, UV (300 nm–400 nm) or short-wavelength (380 nm–440 nm) channel of spectral sensitivity in each rhabdom (Marshall et al., 1991a; Cronin et al., 1993; Thoen et al., 2017). Though most adult stomatopod retinas possess R8 cells across the entire eye, some species have regional variation in UV wavelength sensitivity of up to six physiologically distinct classes of cell (Bok et al., 2014, 2018; Thoen et al., 2017). This polychromatic UV sensitivity is achieved through the combination of different visual pigments expressed in the R8 cells themselves and fluorescent filters found in the optical pathway (Marshall and Oberwinkler, 1999; Bok et al., 2014, 2015).

Crustacean R8 cells lie distal to the main rhabdom, directly beneath the crystalline cone and corneal lens (Fig. 1A). In cross section, the cell body of the R8 cell has a four lobed shape with microvilli directed inward to form the central rhabdomal region

* Corresponding author.
E-mail address: marisa.sarah.mcdonald@gmail.com (M.S. McDonald).
[1] Present Address: NRC Research Associate of the National Academies of Sciences, Engineering, and Medicine, 500 Fifth Street N.W., Washington, DC, 20001

https://doi.org/10.1016/j.asd.2023.101251
1467-8039/

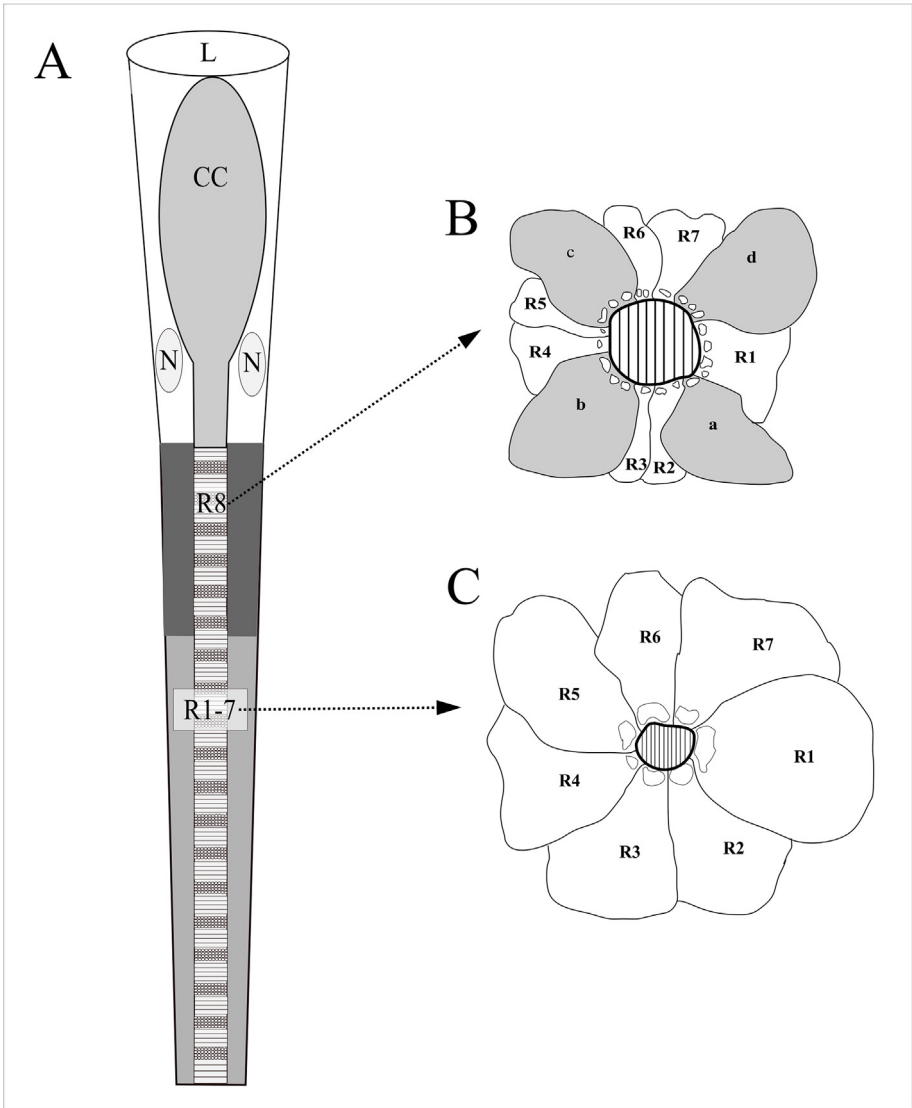

Fig. 1. Schematic drawings of the photoreceptor arrangement in typical crustacean eyes in both longitudinal (**A**), and cross section (**B&C**) orientations. (**A**) Schematic of a typical longitudinal photoreceptor, composed of the lens (L), Crystalline cone structure (CC), crystalline cone cell nuclei (N), and the two-tiered rhabdom, with the distal R8 cell and proximal main rhabdom R1-7. (B) Representative schematic drawing of a cross-section of the R8 photoreceptor shaded in light gray, labeled a-d. (**C**) Schematic of a typical cross section of the main rhabdom with R1-7 labeled (nomenclature from Marshall et al., 1991b).

(Fig. 1B). Within the rhabdom, each R8 cell lobe projects microvilli oriented in one direction such that the microvilli of one lobe meets microvilli from the opposite lobe around the midline (Marshall et al., 1991a). At the level of the R8 cell, thin upward projecting processes from the R1-7 cells can be detected, but do not contribute microvilli to the rhabdom (Marshall et al., 1991b; Feller et al., 2019). In a single ommatidium, the contribution of the R8 cell to the entire rhabdom is relatively small with the majority of the photoreceptive unit being formed from the R1-7 cells (schematic Fig. 1C). R8 cells typically only make up 5–10% of the total rhabdom length in most crustaceans, including the dorsal and ventral hemispheres of adult stomatopod eyes (Marshall et al., 1991a), although the R8 contribution can be up to 25% of the total rhabdom length in ommatidia specialized for detecting polarized light in the stomatopod midband (Marshall et al., 1991a; Templin et al., 2017).

Compared to the specializations described in adult eyes, larval crustacean visual systems are often simpler (Nilsson, 1983; Douglass and Forward, 1989; Cronin and Jinks, 2001; Cronin et al., 2017). Larval decapods, euphausiids, and stomatopods have similar transparent apposition optics and eye structures (Nilsson, 1983). Transparent apposition eyes are composed of elongated crystalline cones that allow for a more tightly packed, less conspicuous, pigmented retina relative to the adult eye. Previous anatomical characterizations of this condensed retina describe the presence of a main rhabdom (R1-7 cells) and a general absence of the R8 cell type (Cronin and Jinks, 2001; Cronin et al., 2017). While R8 cells are documented in the last larval stage of one species of decapod (Douglass and Forward, 1989), prior studies did not find them to be present in earlier stage decapod larvae or to be widespread among crustacean larvae of any type. This was in line with the assumption that specializations for color, UV and polarization vision are not required for mediating behavior in the open ocean pelagic habitats where these larvae are found (Cronin et al., 2017).

While differences in the visual system between adult and larval crustaceans are not uncommon, larval stomatopods stand apart from other crustaceans in their complete replacement of the retina at metamorphosis (Jutte et al., 1998; Feller et al., 2015). Rather than modifying or expanding the larval optical and retinal structures at

metamorphosis, stomatopods develop a completely separate adult retina and optic neuropils that grows adjacent to the existing larval structures (Lin and Cronin, 2018). The larval stomatopod retina is thus completely distinct, both morphologically and physiologically from that of the adult (Cronin et al., 1995; Jutte et al., 1998; Feller and Cronin, 2016). Bolstering this idea of complete separation between adult and larval stomatopod eyes, recent work has identified several optical features unique to larval eyes. The first is a glittery structure or "eyeshine" overlying the pigmented surface of the retina (Feller and Cronin, 2014). The spectral reflectance of larval eyeshine likely assists in camouflaging the conspicuously pigmented retina in open water by matching the background light spectrum (Feller and Cronin, 2014). In addition to eyeshine, one larval stomatopod family was recently identified to have a unique, intrarhabdomal long-wavelength reflecting filter (Feller et al., 2019), which splits photoreceptors in a portion of the eye into multiple tiers, as is often seen in the structure of adult stomatopod rhabdoms (Marshall et al., 1991a, 2007). These findings suggest that larval stomatopods not only have greater structural complexity than previously understood but also are likely to vary both anatomically and physiologically among species.

The arrangement of photoreceptor cells in larval stomatopod retinas remains poorly characterized for most species. Prior studies using microspectrophotometry identified a single sensitivity peak between 450 and 500 nm in multiple species of stomatopod larva (Feller and Cronin, 2016). These studies concluded that larval stomatopods possess a single photoreceptor class provided by the main rhabdoms, composed of the R1-7 cells (Jutte et al., 1998; Cronin and Jinks, 2001; Feller and Cronin, 2016). If larvae possessed a single visual pigment and visual peak sensitivity, this would be expected. However, recent molecular and physiological evidence demonstrated that UV vision is also present in at least one species of larval stomatopod (McDonald et al., 2022). Considering the emerging evidence that larval stomatopods are UV sensitive, we hypothesized that larval stomatopods possess R8 photoreceptor cells in their retinas.

To investigate the presence of R8 cells in stomatopod larval retinas, the retinular cell arrangement was examined in a diverse set of species representing the three most species-rich stomatopod superfamilies: Gonodactyloidea, Lysiosquilloidea, and Squilloidea. Though over 400 species of stomatopod are currently described, almost 80% of the order fall within these three superfamilies (Porter et al., 2010; Van Der Wal et al., 2017). These superfamilies also display remarkable variation in adult eye complexity. Species in the superfamilies Gonodactyloidea and Lysiosquilloidea possess the most complex adult retina type, containing up to 16 anatomically distinct photoreceptor classes in all currently investigated species (Marshall et al., 2007). Adult species in the superfamily Squilloidea, however, have reduced retinal complexity and lack the majority of visual specializations seen in other groups. This evolutionary loss of retinal complexity is attributed to the restricted light habitats the squilloids typically inhabit (Cronin et al., 1993; Marshall et al., 2007; Porter et al., 2009). Variations in adult visual system function are typically associated with differences in light environments and/or ecological needs. In contrast to the habitat diversity seen in the adult stage, all species of larval stomatopods reside in the pelagic open ocean environment and are presumed to have similar ecological needs, largely consisting of avoiding predation, finding food, and eventually identifying appropriate habitat for settling (Cronin et al., 2017). Considering the common demands placed on larval visual systems, it is not unreasonable that previous investigations expected, and sometimes found, strong similarities among species. However, with recent work identifying structural specializations in the eyes of one family of mantis shrimp larvae (Feller et al., 2019) it is possible that structural diversity of the larval stomatopod eye more broadly has been underestimated.

The main focus of this study was to determine if R8 cell anatomical structures allowing for UV vision are present in larval stomatopods across a diverse range of species representing the three main superfamilies. Additionally, we characterized the general organization of visual structures to determine if further structural specializations exist among stomatopod larvae.

2. Methods

2.1. Specimen collection

Larvae from six species representing the three main stomatopod superfamilies were collected for morphological characterizations. Sampling efforts were completed opportunistically at multiple locations using a variety of methods to increase species comparisons. Larval mantis shrimp used in this study were collected and fixed in Florida, Hawai'i, and Australia between July 2017–July 2021 (Table 1). Species were collected using a combination of offshore plankton tows, nighttime shore collections utilizing natural positive phototactic behaviors (Barber and Boyce, 2006; Simpson et al., 2011), and culturing from eggs. None of the species used have had their full larval stages described. However, it is known that larval stomatopods generally undergo an early pro-pelagic stage denotated by a yolk sac, negative phototaxis, and positive thigmotaxis, during which they remain in the adult burrow (Morgan and Goy, 1987; Feller, 2013). Following the pro-pelagic stage (or stages), they enter a series of positively phototactic pelagic stages, in which they are actively feeding. The nature of our collecting methods for wild-caught individuals captured either via light trapping (*Pullosquilla thomassini* and *Alima pacifica)* or Tucker trawling (*Pseudosquilla ciliata*) resulted in the collection of larvae in the pelagic stage of development. The three species of larvae that were lab raised, *Gonodactylaceus falcatus*, *Gonodactylellus* n. sp., and *Pullosquilla* n. sp., were also in the early pelagic stages of development at the time of fixation. This was determined by a loss of yolk sac, positive phototaxis, and active feeding in the lab.

2.2. Species identification

Similar to other studies of stomatopod larvae (Barber et al., 2002; Feller et al., 2013, 2019; Palecanda et al., 2020), COI barcoding was used to identify wild-caught species. Barcode sequencing was completed at the University of Hawai'i at Mānoa. For each individual sample, DNA was extracted using a DNAeasy kit (Qiagen, Hilden, DE, USA) following manufacturer protocols. The cytochrome oxidase I (COI) mitochondrial gene was then amplified through polymerase chain reaction (PCR) using degenerate primers designed for stomatopod COI genes (Palecanda et al., 2020). For each reaction, PCR was conducted using Phire Hot Start Taq (ThermoFisher Scientific, Waltham, MA, USA), following manufacturer protocols with 20 μl total reaction volume and 0.5 μl of 1X forward and reverse primers and 4–8 ng of DNA. For each PCR, the cycling parameters used consisted of a single 2-min incubation at 94 °C; 40 cycles of 20 s 94 °C denaturing, 10 s 46 °C annealing, and 1 min 65 °C elongation; and a final elongation at 65 °C for 7 min.

PCR amplicons were cleaned using EXO-SAP-IT (ThermoFisher Scientific, Waltham, MA, USA) and sequenced in both directions at the Advanced Studies in Genomics, Proteomics, and Bioinformatics facility at the University of Hawai'i at Mānoa (Honolulu, HI, USA). Sequenced chromatograms for each amplicon were assembled (Geneious 10.2.6) and identified using NCBI's Basic Local Alignment Tool (BLAST) (Altschul et al., 1990). Species identification was further verified by alignment of all samples to a curated list of stomatopod reference sequences within the Porter Lab (Steck et al.,

Table 1
Collection details for the species used in this study, including the number of individuals investigated for each species (n), collection location, and collection method.

Superfamily	Species	n	Collection Location	Collection Method
Gonodactyloidea	*Gonodactylaceus falcatus*	3	O'ahu, Hawai'i	Cultured from eggs
	Gonodactylellus n. sp.	2	O'ahu, Hawai'i	Cultured from eggs
	Pseudosquilla ciliata	1	Florida Straits, Florida	Tucker Trawl
Lysiosquilloidea	*Pullosquilla* n. sp.	3	O'ahu, Hawai'i	Cultured from eggs
	Pullosquilla thomassini	2	Lizard Island, Australia	Underwater lights and dipnets
Squilloidea	*Alima pacifica*	2	Lizard Island, Australia	Underwater lights and dipnets

2022). Two species identified and used in this study, *Gonodactylellus* n. sp. and *Pullosquilla* n. sp., are recently discovered Hawaiian species of stomatopod crustaceans that are in the process of being described (Steck et al., 2022).

2.3. Eye tissue preparation

For all species tested, eyes were dissected from live animals under a dissecting microscope by cutting the tissue at the base of the eyestalk and immediately placing it in a fixative composed of 4% gluteraldehyde, 0.1 M sodium cacodylate, and 0.35 M sucrose solution (Weatherby, 1981). For wild caught animals, the remaining body was placed in 100% ethanol for identification using DNA barcoding (Palecanda et al., 2020). After eyes were placed in fixative, they were left at room temperature for 1–2 h before being stored at 4 °C until post-fixation.

To ensure preservation of eye structures, an extended post-fixation protocol was used over the course of three days. Samples were first washed in a 0.1 M cacodylate, 0.44 M sucrose solution 2 × 20 min before being placed in a 1% Osmium tetroxide, 0.1 M cacodylate buffer for 1 h. The samples were then dehydrated in a graded ethanol series at three changes of 5 min, 5 min, and then a final 10-min change. Ethanol was then substituted with propylene oxide three times with changes every 10 min and left in a one part propylene oxide: one part LX112 epoxy resin (Ladd) overnight. The following day, samples were infiltrated with 100% LX112 epoxy resin over a three-day period with 1–2 daily resin changes. Samples were embedded in LX112 epoxy resin blocks and polymerized in an oven (60 °C for 72 h).

2.4. Transmission electron microscopy

Sectioning was completed on an ultramicrotome (Reichert Ultracut E) with a diamond knife. Both semithin sections and serial ultrathin sections were used. Semithin sections (0.5 μm) were used to determine locations in the eye for TEM imaging. Semithin sections were mounted on glass slides, stained with Richardson's stain, and examined on a light microscope. As larval stomatopods have nearly spherical transparent apposition eyes, when sectioning from any angle crystalline cone cross sections would typically be observed first, leading to the top of the rhabdom.

Ultrathin (~80 nm) sections of the larval stomatopod eyes were then cut and collected intermittently on pre-prepared formvar coated slot 1x2 grids for visualization in the TEM. At the point where the crystalline cone tip gives way to the rhabdom, rhabdom cross-sections were examined to look for the presence of an R8 cell. Sectioning continued through the eye to visualize the main rhabdom (cells R1-7) in cross section. Sectioning then continued until the eye gave way to longitudinal sections from ommatidia elsewhere in the eye. All ultrathin sections were visualized and imaged on a TEM (120 kV Hitachi HT7700, AMT XR-41 2048 x 2048 pixel bottom-mount CCD camera or AMT BioSprint16 CCD camera). The cross sectional diameter and area of a minimum of 10 individual rhabdoms for each species and type of section were measured with Image J (Schindelin et al., 2012; Brodrick et al., 2020). All TEM imaging was completed at the Pacific Bioscience Research Center Biological Electron Microscopy Facility.

3. Results

In this study, the optical and photoreceptor structures of three species from Gonodactyloidea, two species from Lysiosquilloidea, and one species from Squilloidea were investigated (Table 1). All species had the same basic stalked eye structure, composed of a near spherical transparent apposition eye typical of other larval crustaceans (Nilsson, 1983). Each individual ommatidium was composed of a lens, crystalline cone light guide, reflective structures creating the characteristic 'eyeshine', and a condensed retina containing retinular and pigment cells, with each structure described in detail below.

3.1. Optical structures

Elongated crystalline cones beneath the corneal lens were present in each of the examined species. The elongated crystalline cone terminated at the image forming rhabdom acting as a light guide for transparent apposition optics. Arthropod crystalline cones are generally composed of four cells (Nilsson 1989), a highly conserved feature in the evolution of arthropod compound eyes resulting in the classification 'Tetraconata' (Richter, 2002; Nilsson and Kelber, 2007). In cross section, larval stomatopod crystalline cones are circular (Fig. 2 C, D) and possess the typical four-cell arrangement expected of this eye type (Fig. 2D). Additionally, an extra cell-like structure was identified along most of the length of the crystalline cone, from beneath the lens to the boundary of the retina (see schematic in Fig. 2A). The structure appeared rectangular in longitudinal sections (Fig. 2B) and was found central to the four main crystalline cone sections along the optical axis when observed in cross-section (Fig. 2C). At the proximal base of the crystalline cone, at the junction with the retina, the typical four cell arrangement of the crystalline cone reemerged, suggesting the central structure is positioned more distal within the dioptric apparatus (Fig. 2D).

The structures responsible for "eyeshine" were observed in all species tested. The eyeshine structures observed in TEM sections (Fig. 3) were composed of layers of subphotonic sized vesicles (~100-200 nm diameter) found at the junction of the crystalline cones and the pigmented retina. These vesicles overlay the retina, but do not cross the light path, as can be seen in gaps in the vesicle structures allowing the crystalline cones to reach the rhabdoms unimpeded (Fig. 3B). Eyeshine is not likely to provide a visual function, as it is not found in the optical pathway of light to the photoreceptors. Instead, the eyeshine reflects light back out of the eye and is hypothesized to assist in camouflage in the open ocean (Feller and Cronin, 2014).

3.2. Retinular cells

All species studied had clear evidence of an R8 photoreceptor cell, in both cross and longitudinal sections. The retinal design observed in each superfamily is described in more detail below.

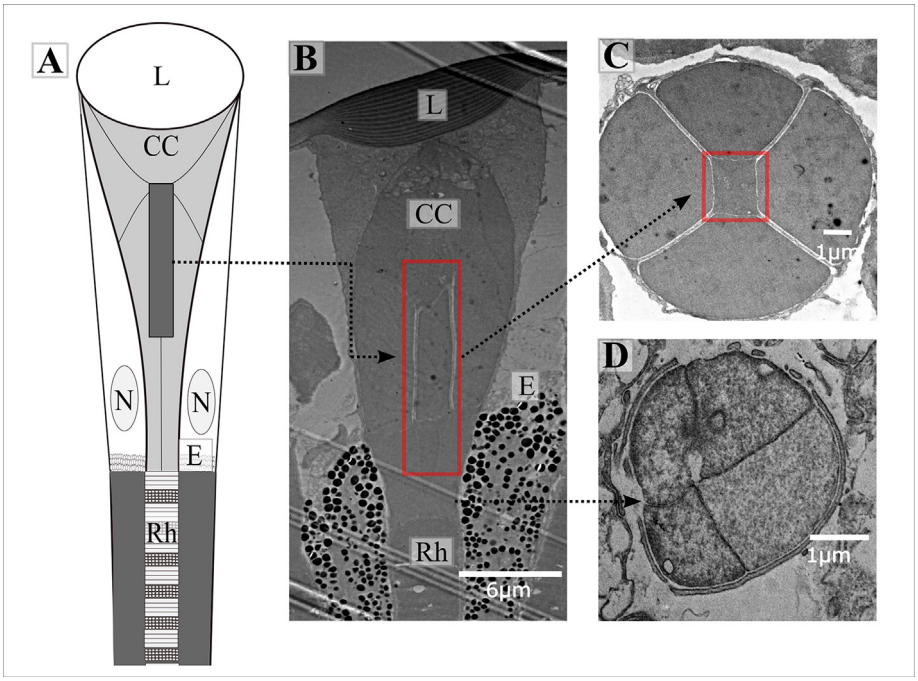

Fig. 2. Representative images of larval stomatopod crystalline cone structures in *Alima pacifica*. (**A**) Schematic of a larval stomatopod ommatidium, depicting the lens (L), crystalline cone (CC), crystalline cone cell nuclei (N), eyeshine structure (E), and rhabdom (Rh); the newly discovered structure is represented by the dark grey rectangle in the crystalline cone. (**B**) Representative electron micrograph of a longitudinal section of the crystalline cone structure in a larval stomatopod, with the unknown structure outlined in red for clarity. (**C**) Electron micrograph of the crystalline cone structure in cross section, located in the center of the four crystalline cone cells and outlined in red for clarity. (**D**) Electron micrograph of the proximal portion of the crystalline cone, showing a more typical arrangement of the four cone cells.

3.2.1. Gonodactyloidea and Squilloidea

Since similar retinal structures were observed in all investigated species from Gonodactyloidea and Squilloidea, these two superfamilies will be considered together. Each larval retina was two-tiered and composed of eight retinular cells, with an R8 photoreceptor distal to a main rhabdom composed of seven retinular cells, R1-7 (see schematic in Fig. 1A). This follows the retinular cell arrangement of typical adult crustaceans, including ommatidia in the dorsal and ventral hemispheres of adult stomatopod eyes (Marshall et al., 1991b; Alkaladi and Zeil, 2014; Brodrick et al., 2020). In all species examined, the R8 cell met the proximal tip of the crystalline cone (Fig. 4B–G). In longitudinal sections, retinular cell bodies are difficult to differentiate and thus the R8 cell was identified as the distal region of unidirectional microvilli bordered on one edge by the crystalline cone cells (Fig. 4B–G). The longitudinal R1-7 cells were characterized by uniform banding of the microvilli (Fig. 4H–M). We were unable to take longitudinal measurements of full rhabdom length vs. R8 cell length in all species studied. However, in the two species that measurements were completed, *G. falcatus* and *Gonodactylellus* n. sp., the R8 cell was estimated to compose approximately 5% of the total rhabdom length, with full rhabdoms measuring at 78.4 μm ± 2.5 um and the R8 cell 3.76 ± 0.2 μm.

The R8 photoreceptor was most easily distinguished in cross-section, in which the individual processes of all retinular cells can be seen (schematic in Fig. 1B). Cross sectional evidence of R8 cells was abundant for each species investigated (Fig. 5 A-C, G-I). The retinular cells of the main rhabdom are composed of seven cells, R1-7. In cross section, these seven cells can be clearly identified in all species (Fig. 5 D-F, J-L). In most species, the diameter of the rhabdom was slightly wider in the R8 cells than in the main rhabdom (Table 2).

3.2.2. Lysiosquilloidea

In the two species from Lysiosquilloidea studied, *Pullosquilla thomassini* and *Pullosquilla* n. sp, the retinular cell arrangement in the dorsal portion of the eye was the same as the other two superfamilies, with a two-tiered rhabdom composed of an R8 cell (Fig. 4E, F; Fig. 5G, H) and a main rhabdom tier composed of R1-7 (Fig. 4K and L, Fig. 5J and K). These two species belong to the Nannosquillidae, which is a family whose larvae are known to contain a specialized intrarhabdomal structural reflector (ISR) in ventrally positioned ommatidia that is associated with tiering of the main rhabdom (Feller et al., 2019). In this study we verified the ISR previously documented in *Pullosquilla thomassini* (Feller et al., 2019), and additionally documented presence of this structure in a new nanosquillid species, *Pullosquilla* n. sp. (Fig. 6), a recently discovered species in Hawai'i in the process of being described (Steck et al., 2022). In photoreceptors that contain the ISR, the main rhabdom R1-7 is split into a proximal tier composed of four cells and distal tier of three cells with the ISR resting in the middle (Feller et al., 2019). The ISR of *Pullosquilla* n. sp. had similar dimensions to ISRs described in other Nanosquillid species, with an average length of 12.29 μm ± 0.45 μm and width of 4.79 μm ± 0.29 μm. The presence of the ISR, subsequently, creates a three-tiered rhabdom in the ventral portion of the retina, composed of the R8 cell microvilli, a distal main rhabdom tier formed by microvillar projections from R1, 4 & 5 cells, and a proximal tier formed by R2, 3, 6, & 7 cells (schematic Fig. 6A, described in Feller et al., 2019).

4. Discussion

Visual system morphological and physiological specializations provide adult stomatopod crustaceans with a unique diversity of color, UV, and polarization visual sensitivity (Marshall et al., 1991a, 1991b; Schiff et al., 2007). Prior studies of stomatopod larval eyes, by comparison, noted the lack of adult specializations in the larvae, suggesting evolution of crustacean larval eyes has generally led to similar eye structures best suited for life in the pelagic habitat (Cronin et al., 1995; Jutte et al., 1998; Feller and Cronin, 2016). In

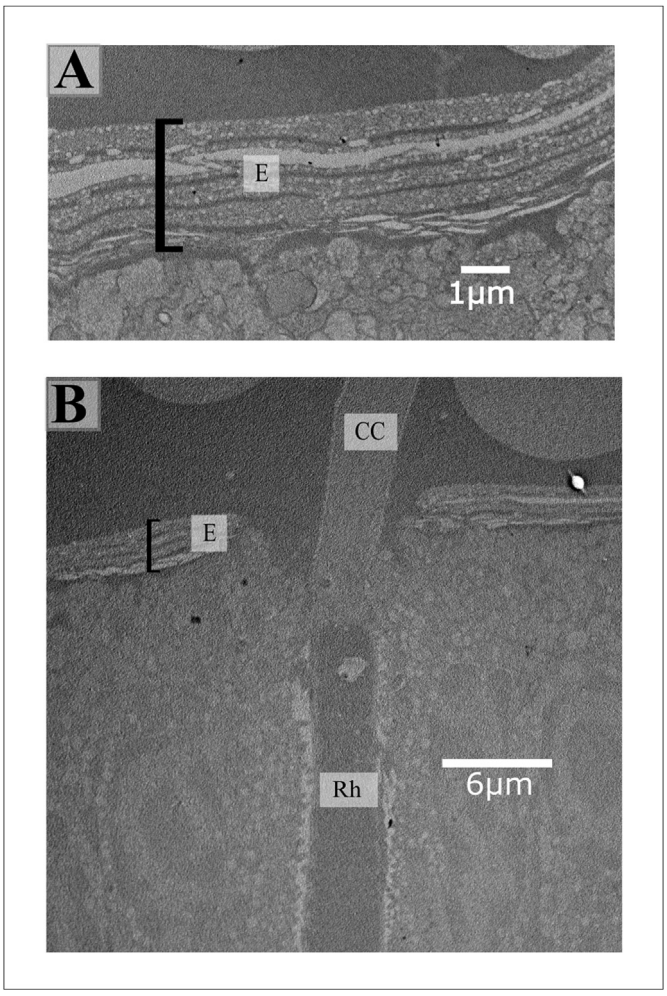

Fig. 3. Structural eyeshine in a larval *Pseudosquilla ciliata*. (**A)** Close-up image of the ordered vesicle structures producing reflective 'eyeshine' (E). **(B)** Longitudinal section of an ommatidium where the base of the crystalline cone (CC) meets the rhabdom (Rh) demonstrating that the eyeshine structure (E) does not disrupt the path of light to the rhabdom.

this study, our close examination of larval stomatopod eyes reveals that both diversity and specialization of optical and retinal structures is greater than previously characterized.

4.1. Crystalline cone structures

Transparent apposition eyes are typical in euphausiid, decapod, and stomatopod larvae. A hallmark feature of transparent apposition eye structures is the extended length of the crystalline cones. In a typical apposition eye, the crystalline cone structures extend a short distance, relative to the total size of the eye, from the corneal lens to the retina (Nilsson, 1989). Additionally, screening pigments migrate between crystalline cones to adjust the sensitivity of an ommatidium to different lighting conditions or times of day (Schönenberger et al., 1980; Halberg& Elofsson, 1989). In transparent apposition eyes, there is no pigmentation between the crystalline cones to maximize transparency of the eye; instead, refractive index gradients act to optically isolate each ommatidium (Nilsson, 1983; Nilsson et al., 1986; Nilsson, 1996).

In this study, we identified a unique anatomical arrangement in the crystalline cones of larval stomatopods. Central to the typical four cell crystalline cone lies a fifth membrane-bound structure (Fig. 2B), the optical significance of which is currently unknown. This structure appears to be ubiquitous among stomatopod larvae as it was identified in each of the species examined in this study. We hypothesize that this structure may be used to establish the refractive gradient necessary for the transparent apposition optical system, allowing on-axis light to reach the rhabdom while reducing off axis light (Nilsson, 1983; Nilsson et al., 1986). The location of the structure along the optical axis and its termination at the boundary of the eyeshine and pigment layer lend support to this hypothesis. Alternatively, this structure may act as a lens cylinder. In butterflies a portion of the crystalline cone acts as a lens to magnify and focus the image onto the rhabdom (Nilsson et al., 1988); the extended crystalline cone structure in larval stomatopods may serve a similar function. Optical measurements of stomatopod larval crystalline cones are required to test these two hypotheses and determine the optical performance of the larval stomatopod crystalline cone structure, or if it confers an optical advantage at all. Additional work is also needed to identify the origin of the material as either a fifth cone cell or a secretion from the lens or cone cells themselves.

4.2. Putative R8 photoreceptor

Larval R8 photoreceptors were identified in each of the species studied, which represent the three main superfamilies: Lysiosquilloidea, Gonodactyloidea, and Squilloidea. Lysiosquilloids and gonodactyloids have the most complex stomatopod adult eyes, with the majority of structural complexity for polarization, color, and UV sensitivity found in a specialized region of the eye known as the midband (Cronin and Marshall, 1989; Marshall et al., 1991a, 2007; Kleinlogel et al., 2003). Squilloid eyes lack the majority of these specializations, exemplified by a reduced midband and electrophysiological studies of adult squilloid species that report a single spectral class of photoreceptor (Cronin et al., 1993). In squilloids, the R8 cells are anatomically present, but generally located proximal to the main rhabdom, rather than distal, and are not believed to be functional (Cronin et al., 1993). However, because the larval retina is distinct from the adult retina, such differences in adult retinal morphology are not expected in larvae.

We found R8 photoreceptor cells in the distal portion of the retina in each larval species examined. While physiological and behavioral evidence suggests the presence of UV vision in a few larval decapod species (Forward and Cronin, 1979; Forward, 1987; Ziegler et al., 2010), few studies have directly investigated larval crustacean eyes for the presence of R8 photoreceptor cells. Prior anatomical characterizations of larval crustacean retinular structures suggest that R8 cells are either absent (Jutte et al., 1998), or absent from early stage larval eyes, emerging only in the penultimate or ultimate stages (Douglass and Forward, 1989). Our study demonstrates that R8 photoreceptor cell morphology is strongly represented in a range of stomatopod taxa, supporting the hypothesis that R8 cells mediate UV visual sensitivity in pelagic stages of stomatopod larvae. This study presents evidence that R8 photoreceptors are present in the larval eyes of a taxonomically diverse set of stomatopods, despite differences among the adult eye morphologies of these groups. At this time, physiological UV sensitivity is known for both gonodactyloid and lysiosquilloid larvae (McDonald, 2022; McDonald et al., 2022). Though physiological sensitivity has yet to be tested in squilloid larvae, the presence of distal R8 cells suggests that these retinas are also sensitive to UV light. Future electrophysiological studies are required to test this hypothesis, since it is possible that these cells may be present but nonfunctional, as is seen in the adults (Cronin et al., 1993).

4.3. Intrarhabdomal structural reflector

While the larval R8 cell and crystalline cone arrangements were

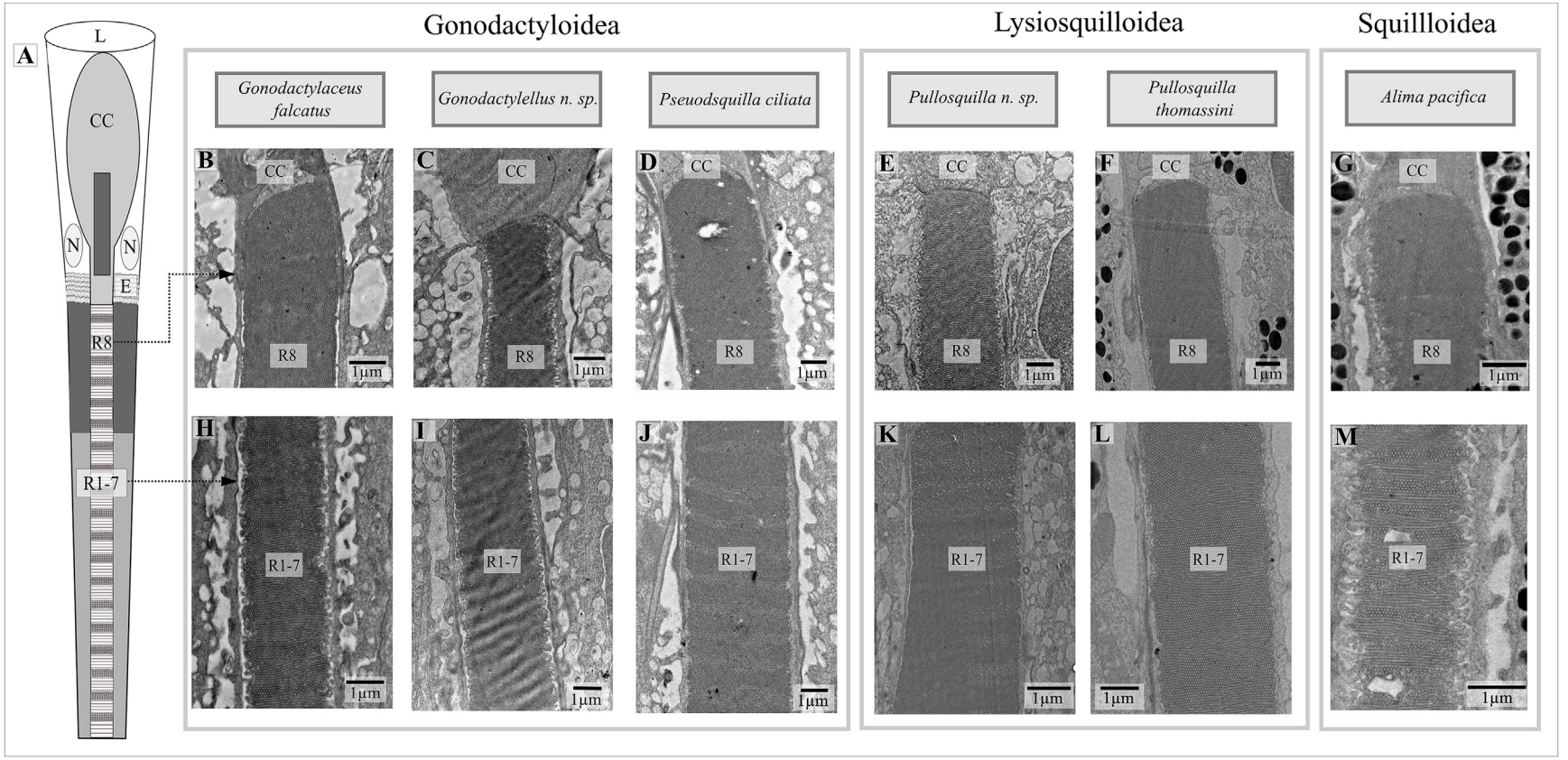

Fig. 4. Overview of the longitudinal arrangement of the rhabdomeric cells in larval stomatopods from the six species tested. (**A)** Schematic drawing of a longitudinal section of a larval stomatopod ommatidium, with the lens (L), crystalline cone (CC), crystalline cone cell nuclei (N), eyeshine structure (E), R8 photoreceptor (R8), and main rhabdom (R1-7) labeled. (**B-G)** Electron micrographs of the longitudinal R8 photoreceptor in each of the characterized species, showing where the proximal end of the crystalline cone (CC) meets the retinular R8 photoreceptor, characterized by microvilli extending in a single direction. (**H-M)** Longitudinal micrographs for each of the characterized species through the R1-7 rhabdom, characterized by evenly sized alternating bands of orthogonally arranged microvilli.

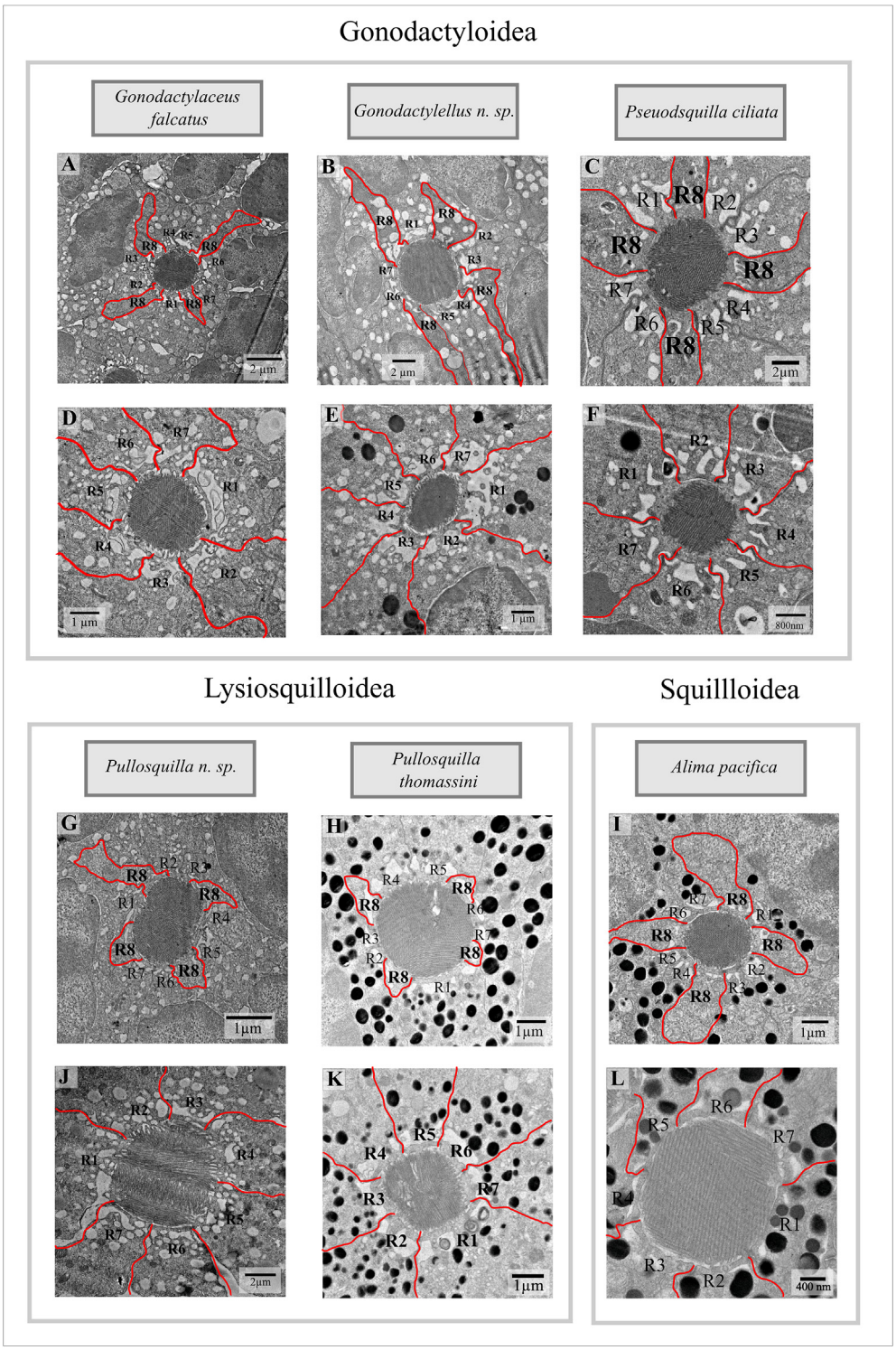

Fig. 5. Overview of retinular cell arrangements in cross-section in each of the species investigated. (**A-C, G-I)** Cross-sections through the retinular R8 cells, with the four lobes of the R8 labeled and outlined for clarity. The cell projections of R1-7 cells are also labeled. (**D-F, J-L)** Cross sections through the medial rhabdom retinular R1-7 cells are displayed, labeled, and outlined for clarity.

common among species, we observed other ommatidial specializations that differ by lineage. Similar to previous work (Feller et al., 2019), we identified an intrarhabdomal structural reflector with a tiered main rhabdom in two species from the family Nannosquillidae, *Pullosquilla thomassini* and *Pullosquilla* n. sp. (Fig. 6). The ISR is thought to be unique to larval stomatopods in the family Nannosquillidae (Feller et al., 2019). Prior to this study, six species were known to possess ISRs in their larval retinas, including one of the species investigated here, *Pullosquilla thomassini*. Our study adds a seventh species to the list, *Pullosquilla* n. sp., bolstering current evidence that the ISR specializations are a unique feature of nanosquillid larval retinas. Previous characterizations of the ISR

Table 2
Measurements of the diameter of cross-sectional samples of microvilli in each of the species tested, given as the average ± s.e.m. Measurements were taken for cross sections both at the level of the R8 photoreceptor cell and in the main rhabdom, with a minimum of 10 cross-sections measured for each rhabdom level and species.

Superfamily	Species	R8 Diameter (μm)	R1-7 Diameter (μm)
Gonodactyloidea	*Gonodactylaceus falcatus*	3.513 ± 0.101	2.643 ± 0.074
	Gonodactylellus n. sp.	2.379 ± 0.060	2.002 ± 0.106
	Pseudosquilla ciliata	1.624 ± 0.032	2.317 ± 0.103
Lysiosquilloidea	*Pullosquilla* n. sp.	3.654 ± 0.096	3.575 ± 0.392
	Pullosquilla thomassini	4.100 ± 0.067	3.277 ± 0.173
Squilloidea	*Alima pacifica*	2.437 ± 0.089	3.054 ± 0.152

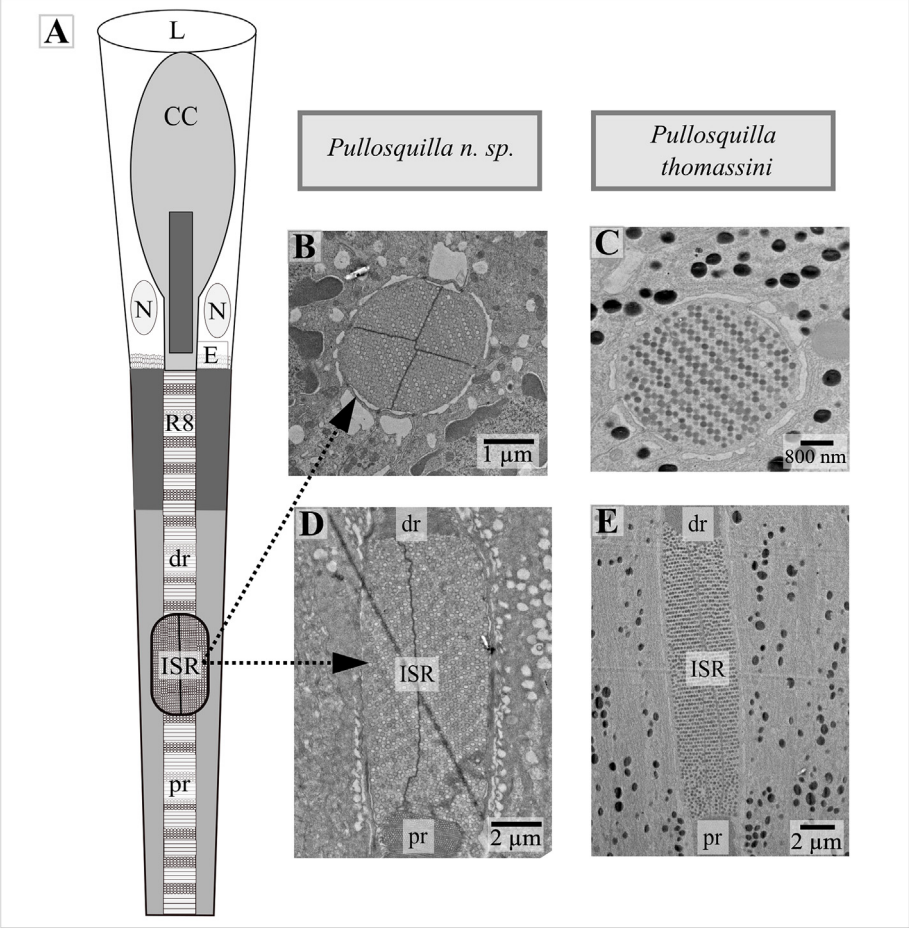

Fig. 6. Representative images of the intrarhabdomal structural reflector (ISR) identified in two of the species studied, *Pullosquilla* n. sp. and *Pullosquilla thomassini*. (**A**) Schematic of the Nannosquillidae rhabdom structure, composed of the lens (L), crystalline cone structure (CC), crystalline cone cell nuclei (N), eyeshine structure (E), and the three-tiered rhabdom composed of the distal R8 cell and the two-tiered main rhabdom divided by the intrarhabdomal structural reflector (ISR) into the distal (dr) and proximal (pr) regions. (**B**) and (**C**) Electron micrographs displaying cross sections of the observed ISR, while (**D**) and (**E**) display longitudinal sections.

demonstrate that it reflects yellowish, long-wavelengths of light (reflectance λ_{max} 548.9–585.5 nm). The size and regular arrangement of the nano-spheres contained within the ISR of *Pullosquilla* n. sp. (Table 3) suggest a similar reflectance would be produced from axial illumination down the ommatidium, though such data were not collected in our study. Considering physiological sensitivity measurements from *Pullosquilla* n. sp. peaked at 602 nm (McDonald, 2022), we predict that nannosquillids have a dominant spectral sensitivity in the long wavelength portion of the spectrum, and that peak sensitivity varies based on the performance of the reflecting filter. Additional studies are needed to test the physiological impact of this structure on larval visual performance.

4.4. Summary and future directions

The sensory ecology of invertebrate marine larvae is an understudied, often overlooked area of research. This paper and other recent work (Feller et al., 2019; McDonald et al., 2022) clearly demonstrate that close examination of such tiny, transparent creatures is ripe with discovery. Our careful examination of the basic structure and anatomy of larval eyes revealed a surprising amount of diversity, suggesting that there is likely more to learn from such organisms. In this study we identified R8 photoreceptors in six taxonomically diverse species of stomatopod larvae suggesting that R8 photoreceptor cells, and therefore UV vision, is widespread among these pelagic zooplankton. Additionally, we

Table 3
Measurements of the intrarhabdomal structural reflector in the two nanosquillid species studied, *Pullosquilla* n. sp. and *Pullosquilla thomassini*. A minimum of five structures were measured for length and width measurements, and a minimum of 100 vesicle diameters were taken to obtain these measurements.

Species	ISR Length (μm)	ISR Diameter (μm)	ISR Vesicle Diameter (nm)
Pullosquilla n. sp.	12.29 ± 0.45	4.79 ± 0.29	153.79 ± 0.9
Pullosquilla thomassini	14.78 ± 0.7	4.09 ± 0.14	153.97 ± 0.87

found a novel crystalline cone structure in larval stomatopod crustaceans (Fig. 2) and confirmed the presence of an intrarhabdomal structural reflector in a seventh species of nanosquillid larvae, strengthening the conclusion that the ISR is a unique feature of this family (Fig. 6) (Feller et al., 2019). Future studies are needed to understand how both UV vision and such specialized optical structures are used by pelagic larvae in their natural environment. This work adds an exciting new chapter to the continually evolving story of unique features in stomatopod visual systems, offering new questions about the role of crustacean larval visual systems as a whole.

Funding

This work was supported by the Graduate Student Organization of the University of Hawaiiānoa and the Crustacean Society Fellowship in Graduate Studies awarded to M.S.M., as well as National Science Foundation DEB (1556105) and EPSCoR RII (1738567) grants to M.L.P. Acquisition of the Hitachi HT7700 Transmission Electron Microscope was funded by the National Science Foundation Grant DBI-1040548 and the Office of the Vice Chancellor for Research and Graduate Education of the University of Hawai'i at Mānoa.

Author statement

Marisa S. McDonald: Conceptualization, Investigation, Writing-Original Draft, Funding Acquisition.
Kathryn D. Feller: Conceptualization, Validation, Writing-Review & Editing.
Megan L. Porter: Resources, Writing-Review & Editing, Supervision, Funding Acquisition.

Acknowledgements

I would like to extend a huge thank you to Tina Weatherby-Carvalho at the Pacific Bioscience Research Center Biological Electron Microscopy Facility. This project would not have been possible without her expertise and guidance. We would like to thank R. Caldwell for sharing his expertise in collecting larval stomatopods, along with L. Vail, A. Hoggett, field assistants too numerous to name, and the staff of the Lizard Island Research Station for support during field work. This is publication #183 from the School of Life Sciences, University of Hawai'i at Mānoa.

Abbreviations

ISR	Intrarhabdomal structural reflector
TEM	Transmission electron microscopy
UV	Ultraviolet
BLAST	Basic Local Alignment Tool
BEMF	Pacific Bioscience Research Center Biological Electron Microscopy Facility

References

Alkaladi, A., Zeil, J., 2014. Functional anatomy of the fiddler crab compound eye (*Uca vomeris*: ocypodidae, Brachyura, Decapoda). J. Comp. Neurol. 522, 1264–1283.
Altschul, S.F., Gish, W., Miller, W., Myers, E.W., Lipman, D.J., 1990. Basic local alignment search Tool. J. Mol. Biol. 215, 403–410.
Barber, P.H., Palumbi, S.R., Erdmann, M.V., Moosa, M.K., 2002. Sharp genetic breaks among populations of *Haptosquilla pulchella* (Stomatopoda) indicate limits to larval transport: patterns, causes, and consequences. Mol. Ecol. 11, 659–674.
Bok, M.J., Porter, M.L., Cronin, T.W., 2015. Ultraviolet filters in stomatopod crustaceans: diversity, ecology and evolution. J. Exp. Biol. 218, 2055–2066.
Bok, M.J., Porter, M.L., Place, A.R., Cronin, T.W., 2014. Biological sunscreens tune polychromatic ultraviolet vision in mantis shrimp. Curr. Biol. 24, 1636–1642.
Bok, M.J., Roberts, N.W., Cronin, T.W., 2018. Behavioural evidence for polychromatic ultraviolet sensitivity in mantis shrimp. Proc. R. Soc. B Biol. Sci. 285.
Brodrick, E.A., Roberts, N.W., Sumner-Rooney, L., Schlepütz, C.M., How, M.J., 2020. Light adaptation mechanisms in the eye of the fiddler crab *Afruca tangeri*. J. Comp. Neurol. 1–19.
Cronin, T.W., Bok, M.J., Lin, C., 2017. Crustacean larvae—vision in the plankton. Integr. Comp. Biol. 57, 1139–1150.
Cronin, T.W., Bok, M.J., Marshall, N.J., Caldwell, R.L., 2014. Filtering and polychromatic vision in mantis shrimps: themes in visible and ultraviolet vision. Philos. Trans. R. Soc. B Biol. Sci. 369, 20130032.
Cronin, T.W., Jinks, R.N., 2001. Ontogeny of vision in marine crustaceans. Am. Zool. 41, 1098–1107.
Cronin, T.W., Marshall, N.J., 1989. Multiple spectral classes of photoreceptors in the retinas of gonodactyloid stomatopod crustaceans. J. Comp. Physiol. 166, 261–275.
Cronin, T.W., Marshall, N.J., Caldwell, R.L., 1993. Photoreceptor spectral diversity in the retinas of squilloid and lysiosquilloid stomatopod crustaceans. J. Comp. Physiol. A. 172, 339–350.
Cronin, T.W., Marshall, N.J., Caldwell, R.L., Pales, D., 1995. Compound eyes and ocular pigments of crustacean larvae (stomatopoda and decapoda, brachyura). Mar. Freshw. Behav. Physiol. 26, 219–231.
Douglass, J.K., Forward, R.B., 1989. The ontogeny of facultative superposition optics in a shrimp eye: hatching through metamorphosis. Cell Tissue Res. 258, 289–300.
Feller, K.D., 2013. Subclass hoplocarida calman, 1904: order stomatopoda latreille, 1817: larvae. In: von Vaupel Klein, J.C., Charmantier-Daures, M., Schram, F.R. (Eds.), Treatise on Zoology-Anatomy, Taxonomy, Biology: the Crustacea, 4A. Brill, Leiden, Netherlands, pp. 257–269.
Feller, K.D., Cohen, J.H., Cronin, T.W., 2015. Seeing double: visual physiology of double-retina eye ontogeny in stomatopod crustaceans. J. Comp. Physiol. A Neuroethol. Sensory, Neural, Behav. Physiol. 201, 331–339.
Feller, K.D., Cronin, T.W., 2014. Hiding opaque eyes in transparent organisms: a potential role for larval eyeshine in stomatopod crustaceans. J. Exp. Biol. 217, 3263–3273.
Feller, K.D., Cronin, T.W., 2016. Spectral absorption of visual pigments in stomatopod larval photoreceptors. J. Comp. Physiol. A Neuroethol. Sensory, Neural, Behav. Physiol. 202, 215–223.
Feller, K.D., Cronin, T.W., Ahyong, S.T., Porter, M.I., 2013. Morphological and molecular description of the late-stage larvae of alima leach, 1817 (crustacea: stomatopoda) from lizard island, Australia. Zootaxa 3722, 22–32.
Feller, K.D., Wilby, D., Jacucci, G., Vignolini, S., Mantell, J., Wardill, T.J., Cronin, T.W., Roberts, N.W., 2019. Long-wavelength reflecting filters found in the larval retinas of one mantis shrimp family (Nannosquillidae). Curr. Biol. 29, 1–8.
Forward, R.B., 1987. Comparative study of crustacean larval photoresponses. Mar. Biol. 94, 589–595.
Forward, R.B., Cronin, T.W., 1979. Spectral sensitivity of larvae from intertidal crustaceans. J. Comp. Physiol. 133, 311–315.
Hallberg, E., Elofsson, R., 1989. Construction of the pigment shield of the crustacean compound eye : a review. J. Crustac Biol. 9, 359–372.
Jutte, P.A., Cronin, T.W., Caldwell, R.L., 1998. Photoreception in the planktonic larvae of two species of pullosquilla, a lysiosquilloid stomatopod crustacean. J. Exp. Biol. 201, 2481–2487.
Kleinlogel, S., Marshall, N.J., Horwood, J.M., Land, M.F., 2003. Neuroarchitecture of the color and polarization vision system of the stomatopod Haptosquilla. J. Comp. Neurol. 467, 326–342.
Lin, C., Cronin, T.W., 2018. Two visual systems in one eyestalk: the unusual optic lobe metamorphosis in the stomatopod *Alima pacifica*. Dev. Neurobiol. 78, 3–14.
Marshall, J., Carleton, K.L., Cronin, T., 2015. Colour vision in marine organisms. Curr. Opin. Neurobiol. 34, 86–94.
Marshall, J., Cronin, T.W., Kleinlogel, S., 2007. Stomatopod eye structure and function: a review. Arthropod Struct. Dev. 36, 420–448.
Marshall, J., Oberwinkler, J., 1999. The colourful world of the mantis shrimp. Nature 401, 873–874.
Marshall, N.J., Land, M.F., King, C.A., Cronin, T.W., 1991a. The compound eyes of

mantis shrimps (Crustacea, Hoplocarida, Stomatopoda). I. Compound eye structure: the detection of polarized light. Philos. Trans. R. Soc. B Biol. Sci. 334, 33–56.
Marshall, N.J., Land, M.F., King, C.A., Cronin, T.W., 1991b. The compound eyes of mantis shrimps (Crustacea , Hoplocarida , Stomatopoda). II. Colour pigments in the eyes of stomatopod crustaceans : polychromatic vision by serial and lateral filtering. Philos. Trans. R. Soc. B Biol. Sci. 334, 57–84.
McDonald, M.S., 2022. Ultraviolet Vision in Larval Stomatopod Crustaceans: Anatomy, Physiology, and Behavior ([Doctoral Dissertation, University of Hawai'I at Mānoa]. Proquest Dissertations and Theses Global).
McDonald, M.S., Palecanda, S., Cohen, J.H., Porter, M.L., 2022. Ultraviolet vision in larval *Neogonodactylus oerstedii*. J. Exp. Biol. 225.
Morgan, S.G., Goy, J.W., 1987. Reproduction and larval development of the mantis shrimp *Gonodactylus bredini* (Crustacea: stomatopoda) maintained in the laboratory. J. Crustac Biol. 7, 595–618.
Nilsson, D.E., 1996. Eye design, vision and invisibility in planktonic invertebrates. In: Lenz, P., Hartline, D.K., Purcell, J., Macmillan, D. (Eds.), Zooplankton: Sensory Ecology and Physiology. Gordan and Breach, Amsterdam, pp. 149–162.
Nilsson, D.E., 1989. Optics and evolution of the compound eye. In: Facets of Vision, pp. 30–73.
Nilsson, D.E., 1983. Evolutionary links between apposition and superposition optics in crustacean eyes. Nature 302, 818–821.
Nilsson, D.E., Hallberg, E., Elofsson, R., 1986. The ontogenetic development of refracting superposition eyes in crustaceans: transformation of optical design. Tissue Cell 18, 509–519.
Nilsson, D.E., Kelber, A., 2007. A functional analysis of compound eye evolution. Arthropod Struct. Dev. 36, 373–385.
Nilsson, D.E., Land, M.F., Howard, J., 1988. Optics of the butterfly eye. J. Comp. Physiol. 162, 341–366.
Palecanda, S., Feller, K.D., Porter, M.L., 2020. Using larval barcoding to estimate stomatopod species richness at Lizard island, Australia for conservation monitoring. Sci. Rep. 10, 10990.
Porter, M.L., Awata, H., Bok, M.J., Cronin, T.W., 2020. Exceptional diversity of opsin expression patterns in *Neogonodactylus oerstedii* (Stomatopoda) retinas. Proc. Natl. Acad. Sci. U.S.A. 117, 8948–8957.
Porter, M.L., Bok, M.J., Robinson, P.R., Cronin, T.W., 2009. Molecular diversity of visual pigments in Stomatopoda (Crustacea). Vis. Neurosci. 26, 255–265.
Porter, M.L., Zhang, Y., Desai, S., Caldwell, R.L., Cronin, T.W., 2010. Evolution of anatomical and physiological specialization in the compound eyes of stomatopod crustaceans. J. Exp. Biol. 213, 3473–3486.
Richter, S., 2002. The Tetraconata concept: hexapod-crustacean relationships and the phylogeny of Crustacea. Org. Divers. Evol. 2, 217–237.
Schiff, H., Manning, R.B., Abbot, B.C., 2007. Structure and pptics of ammatidia from eyes of stomatopod crustaceans from different luminous habitats. Biol. Bull. 170, 461–480.
Schindelin, J., Arganda-Carreras, I., Frise, E., Kaynig, V., Longair, M., Pietzsch, T., Preibisch, S., Rueden, C., Saalfeld, S., Schmid, B., Tinevez, J.-Y., White, D.J., Hartenstein, V., Eliceiri, K., Tomancak, P., Cardona, A., 2012. Fiji: an open-source platform for biological-image analysis. Nat. Methods 9, 676–682.
Schönenberger, N., Cox, J.A., Gabbiani, G., 1980. Evidence for hemocyanin formation in the compound eye of *Squilla mantis* (Crustacea, Stomatopoda). Cell Tissue Res. 205, 397–409.
Steck, M., Winnicki, E., Kobayashi, D.R., Whitney, J.L., Ahyong, S.T., Porter, M.L., 2022. Hawaiian larval stomatopods: molecular and morphological diversity. Zootaxa 5214, 235–260.
Templin, R.M., How, M.J., Roberts, N.W., Chiou, T.H., Marshall, J., 2017. Circularly polarized light detection in stomatopod crustaceans: a comparison of photoreceptors and possible function in six species. J. Exp. Biol. 220, 3222–3230.
Thoen, H.H., Chiou, T.H., Marshall, N.J., 2017. Intracellular recordings of spectral sensitivities in stomatopods: a comparison across species. Integr. Comp. Biol. 1–13.
Thoen, H.H., How, M.J., Chiou, T.H., Marshall, J., 2014. A different form of color vision in mantis shrimp. Science 343, 411–413.
Van Der Wal, C., Ahyong, S.T., Ho, S.Y.W., Lo, N., 2017. The evolutionary history of Stomatopoda (Crustacea: malacostraca) inferred from molecular data. PeerJ 2017, e3844.
Weatherby, T.M., 1981. Ultrastructural study of the sinus gland of the crab, *Cardisoma carnifex*. Cell Tissue Res. 220, 293–312.
Ziegler, T.A., Cohen, J.H., Forward, R.B., 2010. Proximate control of diel vertical migration in phyllosoma larvae of the Caribbean spiny lobster *Panulirus argus*. Biol. Bull. 219, 207–219.